arXiv:2507.04059v1 [cs.LG] 5 Jul 2025

Attributing Data for Sharpness-Aware Minimization

Chenyang Ren[*,1,2], Yifan Jia[*,1,3], Huanyi Xie[*,1,2], Zhaobin Xu[1,3],
Tianxing Wei[1,3], Liangyu Wang[1,2], Lijie Hu[†,1,2], Di Wang[†,1,2]
[1]Provable Responsible AI and Data Analytics (PRADA) Lab
[2]King Abdullah University of Science and Technology
[3]Shandong University

Abstract

Sharpness-aware Minimization (SAM) improves generalization in large-scale model training by linking loss landscape geometry to generalization. However, challenges such as mislabeled noisy data and privacy concerns have emerged as significant issues. Data attribution, which identifies the contributions of specific training samples, offers a promising solution. However, directly rendering existing data influence evaluation tools such as influence functions (IF) to SAM will be inapplicable or inaccurate as SAM utilizes an inner loop to find model perturbations that maximize loss, which the outer loop then minimizes, resulting in a doubled computational structure. Additionally, this bilevel structure complicates the modeling of data influence on the parameters. In this paper, based on the IF, we develop two innovative data valuation methods for SAM, each offering unique benefits in different scenarios: the Hessian-based IF and the Gradient Trajectory-based IF. The first one provides a comprehensive estimation of data influence using a closed-form measure that relies only on the trained model weights. In contrast, the other IF for SAM utilizes gradient trajectory information during training for more accurate and efficient data assessment. Extensive experiments demonstrate their effectiveness in data evaluation and parameter tuning, with applications in identifying mislabeled data, model editing, and enhancing interpretability.

1 Introduction

Over the past decade, deep neural networks have advanced significantly due to increased model parameter sizes and improved training algorithms that enhance generalization. However, larger models often memorize training data, leading to overfitting and poor generalization. In order to address this issue, considerable effort has been invested in the development of a range of strategies, including differential privacy [26, 29, 54, 66, 60, 61, 59, 64], regularization techniques [57, 63, 43] and adversarial training [44, 52, 18, 17, 38, 68]. Recent work has observed that sharp local minima in the loss landscape can significantly impair the generalization performance of deep networks [33, 24, 45]. To make the loss landscape flatter to improve models' generalization ability, [16] introduced a general framework called Sharpness-aware Minimization (SAM). SAM improves generalization by penalizing sharp minima and encouraging convergence to flatter regions. Intuitively, SAM is a bilevel optimization problem, where the inner level seeks weight perturbations that can lead to the maximum loss, which is a measure of local sharpness. On the outer level, the model is trained to minimize both loss and local sharpness simultaneously. Thus, it can also be formulated as a minimax optimization problem. SAM has achieved state-of-the-art results across various tasks [16, 9, 41].

[*]Equal Contribution.
[†]Corresponding Author.

Preprint. Under review.

While SAM has been applied in various real-world applications [14, 2, 48, 4], the presence of noisy data in the training set, including mislabeled or poisoned data, has become a significant concern. A critical approach to tackling this issue involves identifying the contributions of training samples in SAM-trained models by assessing their impact on model performance, a process referred to as (training data) attribution. Data attribution plays a critical role in tracing model outputs back to significant training examples, thereby providing insights into how individual data points influence model performance.

Data attribution has been used in various tasks to enhance model transparency and understanding of how training data influences model behavior [50, 42, 65]. Generally, data attribution methods [32, 19, 62, 22] assign higher contribution scores to training instances that significantly improve model performance when included, which can be divided into two types. The first one, such as Shapley Value [56], is based on sampling [42, 36], which requires multiple retraining with different data subsets. This is computationally expensive and impractical for large models. To address this challenge, the second approach—namely, influence function-based methods [34, 15, 49, 27, 28]—estimates data contributions using gradient information, thereby facilitating accurate assessments without the need for retraining. Recent advancements have led to innovative estimators utilizing the training gradient trajectory [47, 51], which estimate the influence of training data on model predictions by tracing gradient descent, providing better insights into and improvements of training examples in deep learning models. These methods do not depend on the convexity assumption of the loss function, nor do they require computationally intensive Hessian inversions. Instead, they perform calculations based on the training gradient and have achieved good results in many tasks [40].

However, it is essential to note that influence functions were initially designed for M-estimators [30] (i.e., minimizing the summation of loss on all data), which limits their direct applicability to the bilevel structure in SAM. Specifically, the influence of data on perturbations, and consequently on model parameters, is in an indirect manner and has not been considered in classical influence functions. Due to the coupled outer-inner optimization process involved in SAM, any changes to the model parameters will necessitate further updates to the inner perturbations and consequently alter the outer model parameters. Furthermore, in the actual training of SAM, the inner perturbations are not derived through the optimization process but are instead via approximation. To further accelerate computations, the outer gradient descent is also approximated, resulting in minor deviations in the inner perturbations from the original SAM model. These complicate our ability to evaluate the influence of data in SAM accurately.

In this paper, we propose two data valuation methods based on influence functions for SAM, focusing on two distinct scenarios. Firstly, we derive a closed form of the Hessian-based Influence Function (SAM-HIF) from the mathematical formulation of SAM through theoretical derivation. SAM-HIF fully considers the impact of data on the model's local sharpness. In the absence of gradient trajectory information, SAM-HIF serves as a comprehensive estimation method. However, when gradient trajectory information during training is accessible, we can focus on the specific training algorithm to derive a more accurate evaluation method. Inspired by [47], we propose the Gradient Trajectory-based Influence Function (SAM-GIF). This method utilizes checkpoints to evaluate the influence of data within SAM, leading to accurate data assessment while reducing implementation and computational costs. SAM-GIF proves to be highly effective due to its simplicity, high scalability, and accuracy. To sum up, our contributions are listed as follows:

- We present data evaluation methods using influence functions (IF) for SAM and its training algorithms. First, we derive SAM-HIF, which allows for precise modeling of data influence in SAM by effectively capturing influences on both model parameters and model perturbations. Second, we present SAM-GIF for SAM training algorithms, which showcases exceptional precision and scalability when training gradient trajectories are accessible. We also discuss some downstream applications and strategies to accelerate the computation of our influence functions.

- Our method has potential applications in several real-world scenarios, including the automatic identification and removal of potentially harmful data points, SAM model editing, and enhancing the interpretability of SAM-trained models. We validate the effectiveness and efficiency of SAM-HIF and SAM-GIF through comprehensive experimental evaluations. Experimental results indicate that our framework performs well in data evaluation and the tuning of SAM-trained models.

2 Related Work

Sharpness Aware Minimization. The concept of flat minima and its link to reducing overfitting and enhancing model generalization was first explored by [25], establishing a foundation for understanding why models that converge to flatter regions tend to generalize better. Additionally, [33] experimentally examined the relationship between batch size, sharp minima, and generalization. Their findings provided empirical support for SAM's theoretical foundations and highlighted the importance of sharpness in optimization and model training. Overall, sharp local minima can significantly influence the generalization capabilities of deep networks [7, 31]. Building on these insights, one of the foundational works on SAM is by [16], who proposed a bi-level optimization framework that seeks perturbations around model parameters to maximize loss and guide the model towards flatter minima. Recent studies have further explored the behavior SAM. For example, [3] investigated the geometric properties of loss landscapes, demonstrating that SAM's perturbation-based approach offers insights into model behavior. Their findings indicate that SAM not only improves generalization but also enhances understanding of models' sensitivity to input perturbations. [67] assert that SAM [16] is effectively equivalent to applying a gradient norm regularization through the approximation of the Hessian matrix. [35] introduce adaptive sharpness-aware minimization, which can dynamically adjust the maximization region based on the weight scale. To minimize computational costs associated with SAM, [14] introduced Efficient SAM, which randomly computes perturbations.

Influence Function. The influence function(IF), initially developed in robust statistics [10, 11], has become essential in machine learning since its introduction by [34]. IFs have been used to various fields, including interpreting model outputs, reducing model bias [55], and facilitating machine unlearning [39, 21, 20]. Its versatility spans various fields, including natural language processing [22] and image classification [5], while also addressing biases in classification models [55], word embeddings [6], and model fine-tuning [8]. A recent innovative influence function that leverages the training gradient trajectory has been proposed and investigated [47, 51], and has been successfully applied in instructional fine-tuning [58]. Despite the numerous studies related to influence functions, we are the first to use this concept for the data evaluation of models trained for SAM. This provides us with a completely new perspective on understanding the training process of SAM.

3 Preliminaries

Sharpness-Aware Minimization (SAM). SAM presents a novel approach to optimizing machine learning models with the primary objective of enhancing generalization by mitigating the sharpness of the loss landscape. Given a dataset $S = \{(x_i, y_i)\}_{i=1}^n$, we define the training loss associated with model parameters ω and a perturbation ϵ as:

$$L_S(\omega + \epsilon) = \frac{1}{n} \sum_{i=1}^{n} \ell(x_i, y_i; \omega + \epsilon) \triangleq \sum_{i=1}^{n} L_S^i(\omega + \epsilon).$$

Then SAM optimization framework seeks parameters that lie in neighborhoods having uniformly low loss by the following procedure. Firstly, seeking the model perturbation maximizing the loss:

$$\hat{\epsilon}(\omega) = \arg\max_{||\epsilon||_p \leq \rho} L_S(\omega + \epsilon).$$

Then minimize the uniform loss by the following loss function:

$$\omega^* = \arg\min_{\omega} L_S(\omega + \hat{\epsilon}(\omega)) + \frac{\lambda}{2} \cdot ||\omega||_2^2. \tag{1}$$

where λ is the regularization parameter. Here, SAM takes model loss sharpness into consideration via including the perturbation process. The loss function for SAM can be formed into one equation as follows:

$$\begin{aligned} L_S^{SAM}(\omega) =& L_S(\omega + \hat{\epsilon}(\omega)) + \frac{\lambda}{2} \cdot ||\omega||_2^2 \\ =& \max_{||\epsilon||_p \leq \rho} L_S(\omega + \epsilon) + \frac{\lambda}{2} \cdot ||\omega||_2^2. \end{aligned}$$

In essence, SAM seeks to minimize the worst-case loss by enforcing a level of robustness against perturbations in the parameter space, thereby promoting smoother loss landscapes. Besides, the gradient of L_S^{SAM} is calculated by

$$\nabla L_S^{SAM}(\omega) = \nabla L_S(\omega + \hat{\epsilon}(\omega)) + \frac{\mathrm{d}\hat{\epsilon}(\omega)}{\mathrm{d}\omega} \cdot \nabla L_S(\omega + \hat{\epsilon}(\omega)). \tag{2}$$

Influence Function. The influence function [30] quantifies how an estimator relies on the value of each individual point in the sample. Consider a neural network $\hat{\theta} = \arg\min_\theta L(\theta, D) = \sum_{i=1}^n \ell(z_i; \theta)$ with loss function ℓ and dataset $D = \{z_i\}_{i=1}^n$. When an individual data point z_m is removed from the training set, the retrained optimal retrained model is denoted as $\hat{\theta}_{-z_m}$. The influence function method provides an efficient way to approximate $\hat{\theta}_{-z_m}$ without the need of retraining. By up-weighing z_m-related term in the loss function by δ, a series of δ-parameterized optimal models $\hat{\theta}_{-z_m,\delta}$ will be obtained by

$$\hat{\theta}_{-z_m,\delta} = \arg\min_\theta \left[L(\theta, D) + \delta \cdot \ell(z_m; \theta) \right].$$

Consider the term

$$\nabla L(\hat{\theta}_{-z_m,\delta}, D) + \delta \cdot \nabla \ell(z_m; \hat{\theta}_{-z_m,\delta}) = 0, \tag{3}$$

we perform a Taylor expansion at $\hat{\theta}$ and incorporate the optimal gradient condition at $\hat{\theta}_{-z_m}$ and $\hat{\theta}$:

$$\sum_{i=1}^n \nabla \ell(z_i; \hat{\theta}) + \delta \cdot \nabla \ell(z_m; \hat{\theta}) + H_{\hat{\theta}} \cdot \left(\hat{\theta}_{-z_m,\delta} - \hat{\theta} \right) \approx 0$$

where $H_{\hat{\theta}} = \sum_{i=1}^n \nabla_{\hat{\theta}}^2 \ell(z_i; \hat{\theta})$ is the Hessian matrix. Consequently, the Influence Function is defined as the derivative of the change in parameters of the retrained model due to perturbation with respect to the perturbation:

$$\mathrm{IF}(z_m) = \left. \frac{\mathrm{d}\hat{\theta}_{-z_m,\delta} - \hat{\theta}}{\mathrm{d}\delta} \right|_{\delta=0} \approx -H_{\hat{\theta}}^{-1} \cdot \nabla \ell(z_m; \hat{\theta}).$$

When setting $\delta = -1$, this results in the complete removal of z_m from the retraining process. Then, $\hat{\theta}_{-z_m}$ can be approximated by a linear approximation formula as $\hat{\theta} - \mathrm{IF}(z_m)$. Additionally, for a differentiable evaluation function, such as one used to calculate the total model loss over a test set, the change resulting from up-weighting ϵ to z_m in the evaluation results can be approximated as $-\nabla f(\hat{\theta}) \cdot \mathrm{IF}(z_m)$.

4 Evaluating Data Attribution in SAM

To evaluate the influence of an individual data point for SAM, we utilize assessing model differences after leave-one-out (LOO) retraining.

4.1 Evaluating Data Attribution in SAM via Hessian-based IF

To evaluate the influence of an individual data point for the model trained via SAM, we first provide an estimation of the leave-one-out (LOO) retrained model. Then we can quantify the parameter-level influence of the excluded data point by analyzing the differences in model parameters before and after the retraining process. Due to the unique architecture of SAM, the form of the corresponding loss function differs from that of traditional IF. This is because SAM includes an additional step to find parameter perturbations that maximize the loss, which will also change as a result of the LOO retraining process. We provide details in the following.

Definition 4.1 (LOO Retrained Parameter)**.** Consider one data (x_k, y_k) to be evaluated, $\hat{\epsilon}_k(\omega)$ denotes the perturbation around ω which results in the maximum loss after the removal of (x_k, y_k), which is defined as

$$\hat{\epsilon}_k(\omega) = \arg\max_{||\epsilon||_p \leq \rho} \sum_{i \neq k}^n L_S^i(\omega + \epsilon).$$

Then, the LOO retrained model is defined as

$$\omega_k = \arg\min_{\omega} \sum_{i \neq k} L_S^i(\omega + \hat{\epsilon}_k(\omega)) + \frac{\lambda}{2} \cdot ||\omega||_2^2. \tag{4}$$

From the preceding discussion, we denote the influence of the data point (x_k, y_k) on the SAM-trained model as $\omega_k - \omega^*$. To avoid retraining, we utilize the influence function method to approximate this difference. We begin by transforming the optimality condition of (1) into a simpler form via Danskin's Theorem [12].

Lemma 4.2. *The optimal solution w^* of SAM, as represented in (1), satisfies*

$$\nabla L_S(\omega^* + \hat{\epsilon}(\omega^*)) + \frac{\mathrm{d}\hat{\epsilon}(\omega^*)}{\mathrm{d}\omega^*} \cdot \nabla L_S(\omega^* + \hat{\epsilon}(\omega^*)) + \lambda \cdot \omega^* = 0,$$

which is equivalent to the following condition

$$\nabla L_S(\omega^* + \hat{\epsilon}(\omega^*)) = 0.$$

Follow the idea of influence function, we up-weigh the k-th term in the loss function by a factor of δ. This adjustment allows us to derive a series of model parameters $\omega_{k,\delta}$ obtained by training the models via SAM:

$$\begin{aligned}\omega_{k,\delta} = \arg\min L_{\text{Total},\delta}(\omega) \triangleq L_{S,\delta}(\omega) + \frac{\lambda}{2} \cdot ||\omega||_2^2 \\ = L_S(\omega + \hat{\epsilon}_\delta(\omega)) + \delta \cdot L_S^k(\omega + \hat{\epsilon}_\delta(\omega)) + \frac{\lambda}{2} \cdot ||\omega||_2^2\end{aligned}$$

The δ-related term in the loss function directly reflects the influence of (x_k, y_k) on ω. Note that $\omega_{k,-1} = \omega_k$. Additionally, the learning of the worst perturbation is influenced by the up-weighting factor δ, as reflected in the modified objective function for ϵ:

$$\hat{\epsilon}_{k,\delta}(\omega) = \arg\max_{||\epsilon||_p \leq \rho} \left[\sum_{i=1}^{n} L_S^i(\omega + \epsilon) + \delta \cdot L_S^k(\omega + \epsilon) \right]$$

This modification in the objective function, in turn, indirectly influences the optimal parameters learned through SAM. Starting from a simplified case, we neglect the indirect influence of the perturbation and introduce the simplified version of SAM-IF.

Theorem 4.3. *Consider the data (x_k, y_k) along with a SAM-trained model ω^*, $\hat{\epsilon}(\omega^*)$ represents the model weight perturbation that results in the largest loss. Then the corresponding SAM-IF is defined as:*

$$\textit{SAM-IF}(x_k, y_k) = -H_\omega^{-1} \cdot \nabla L_S^k(\omega^* + \hat{\epsilon}(\omega^*))$$

where H_ω is defined as $H_\omega = \nabla^2 L_S\left(\omega^* + \hat{\epsilon}(\omega^*)\right) + \lambda$. ω_k can be approximated by

$$\omega_k \approx \omega^* - \textit{SAM-IF}(x_k, y_k).$$

We can see that in SAM-IF we still use $\hat{\epsilon}(\omega^*)$ in both Hessian matrix and gradient, while the optimal perturbation should be $\hat{\epsilon}_{k,-1}(\omega_k)$. However, neglecting the term related to the perturbation can lead to an incomplete and inaccurate evaluation of data influence. In fact, it implies that while the influence of this data point on the model's loss function is considered, the impact of removing this data point on the computation of model sharpness is not taken into account. This will lead to an incomplete evaluation of data influence. To take this into consideration, $\hat{\epsilon}_{k,\delta}\left(\omega_{k,\delta}\right) - \hat{\epsilon}(\omega^*)$ also need to be estimated, which is given in the following lemma.

Lemma 4.4. *The term $\hat{\epsilon}_{k,\delta}\left(\omega_{k,\delta}\right) - \hat{\epsilon}(\omega^*)$ can be approximated by*

$$\begin{aligned}&\hat{\epsilon}_{k,\delta}(\omega_{k,\delta}) - \hat{\epsilon}(\omega^*) \\ =&\hat{\epsilon}_{k,\delta}(\omega^*) - \hat{\epsilon}(\omega^*) + \left.\frac{\mathrm{d}\hat{\epsilon}_{k,\delta}(\omega)}{\mathrm{d}\omega}\right|_{\omega=\omega^*} \cdot (\omega_{k,\delta} - \omega^*).\end{aligned} \tag{5}$$

When $\epsilon \to 0$, $\hat{\epsilon}_{k,\delta}(\omega^*) - \hat{\epsilon}(\omega^*) \to 0$, then $\hat{\epsilon}_{k,\delta}(\omega_{k,\delta}) - \hat{\epsilon}(\omega^*)$ can be bounded by $\omega_{k,\delta} - \omega^*$, which is especially useful for the following derivation.

Theorem 4.5. *Consider the k-th data (x_k, y_k) along with a SAM-trained model ω^*. Define the Hessian-based influence function for SAM(SAM-HIF) as:*

$$\begin{aligned} &\textit{SAM-HIF}(x_k, y_k) \\ =& -\left(H_\omega + H_\omega \cdot \frac{\mathrm{d}\hat{\epsilon}(\omega^*)}{\mathrm{d}\omega}\right)^{-1} \cdot \nabla L_S^k\left(\omega^* + \hat{\epsilon}(\omega^*)\right). \end{aligned}$$

Then ω_k can be approximated by:

$$\omega_k \approx \omega^* - \textit{SAM-HIF}(x_k, y_k).$$

Note that in general, there is no closed-form solution for the term $\frac{\mathrm{d}\hat{\epsilon}(\omega^*)}{\mathrm{d}\omega}$, to address the issue, we can use the method in [16] to approximate $\hat{\epsilon}$:

$$\hat{\epsilon}(\omega) = \rho \cdot \operatorname{sign}(\nabla_w L_S(\omega, 0)) \cdot \frac{|\nabla_w L_S(\omega, 0)|^{q-1}}{\left(\|\nabla_w L_S(\omega, 0)\|_q^q\right)^{1/p}}, \tag{6}$$

where p satisfies $\frac{1}{p} + \frac{1}{q} = 1$. Based on the assumption that the sign of the gradient $\nabla_w L_S(\omega, 0)$ remains unchanged under the removal of one data point, $\frac{\mathrm{d}\hat{\epsilon}(\omega^*)}{\mathrm{d}\omega^*}$ can be calculated easily.

4.2 Improving Data Valuation via Gradient Trajectory

In Theorem 4.5, we have to know the exact worst perturbation $\hat{\epsilon}(\omega)$. However, according to [16], to accelerate the training, the training algorithm for SAM uses the following closed-form estimation of $\hat{\epsilon}(\omega^*)$ in (6) to replace the procedure of finding the model perturbation that results in the largest loss. Besides, for the outer-level gradient descent, the second term in (2) is intentionally dropped during training for simplification, and the final gradient approximation they use is actually $\nabla L_S(w + \hat{\varepsilon}(w))$. See Algorithm 1 for details. Therefore, the SAM-HIF we proposed based on the minimization condition represents an idealized case, which sometimes proves insufficiently reliable in practical applications where we cannot find the optimal minimizer.

Algorithm 1 SAM Algorithm in [16]

Require: Training set S, Loss function L, Batch size b, Step size $\eta > 0$, Neighborhood size $\rho > 0$.
Ensure: Model trained with SAM
1: Initialize weights w_0, $t = 0$;
2: **while** not converged **do**
3: Sample batch $B = \{(x_1, y_1), \ldots, (x_b, y_b)\}$;
4: Compute gradient $\nabla_w L_{\mathcal{B}}(w_t)$ of batch's training loss;
5: Compute $\hat{\epsilon}(w)$ per Equation (6);
6: Compute gradient: $g = \nabla_w L_B(w_t + \hat{\epsilon}(w_t))$;
7: Update weights: $w_{t+1} = w_t - \eta g$; $t = t + 1$;
8: **end while**

To bridge the gap, we will next focus on the SAM model trained via the canonical training algorithm in [16], where we have the training trajectory stored in checkpoints. To measure the influence of the k-th data in the training dataset, similar to HIF, we firstly define a loss function with the k-th term up-weighted by δ as:

$$L_S(\omega; \delta) = L_S(w) + \delta \cdot L_S^k(\omega). \tag{7}$$

Consider the model trained based on loss function (7) using a gradient descent optimizer in [16]. At training step t, model parameters are updated as

$$\begin{aligned} &\omega_{t,\delta} - \omega_{t-1,\delta} \\ =& -\eta_{t-1} \cdot \nabla_\omega L_S\left(\omega_{t-1} + \hat{\epsilon}(\omega_{t-1})\right) \\ &- \delta \cdot \eta_{t-1} \nabla_\omega L_S^k\left(\omega_{t-1,\delta} + \hat{\epsilon}(\omega_{t-1,\delta})\right), \end{aligned}$$

where η_{t-1} is the learning rate at step $t-1$, and $\hat{\epsilon}(\omega_{t-1}, \delta)$ is defined in (6). Then, the model trained after T steps becomes

$$\omega_{T,\delta} = \omega_0 - \sum_{t=0}^{T-1} \eta_t \cdot \nabla_\omega L_S\left(\omega_{t,\delta} + \hat{\epsilon}(\omega_{t,\delta}); \delta\right).$$

Based on the above discussion, we derive the Gradient-based Influence Function (SAM-GIF) by calculating the derivative of the up-weighted retrained parameter $\omega_{T,\delta}$ for the k-th data point with respect to δ.

$$\begin{aligned}
&\frac{\mathrm{d}\omega_{T,\delta}}{\mathrm{d}\delta}\bigg|_{\delta=0} \\
=&-\sum_{t=0}^{T-1}\eta_t\cdot\frac{\mathrm{d}\nabla_\omega L_S\left(\omega_{t,\delta}+\hat{\epsilon}(\omega_{t,\delta});\delta\right)}{\mathrm{d}\delta}\bigg|_{\delta=0} \\
&-\sum_{t=0}^{T-1}\eta_t\cdot H_{t,0}\cdot\frac{\mathrm{d}(\omega_{t,\delta}+\hat{\epsilon}(\omega_{t,\delta}))}{\mathrm{d}\delta}\bigg|_{\delta=0},
\end{aligned}$$

where $H_{t,0}$ is the Hessian matrix of $L_S(\omega_t)$. To reduce the calculation complexity, we omit the second Hessian term and thus have the following approximation:

$$\text{SAM-GIF}_{\text{GD}}(x_k,y_k)=-\sum_{t=0}^{T-1}\eta_t\cdot\nabla_\omega L_S^k(\omega_t+\hat{\epsilon}(\omega_t)).$$

This definition is consistent with [47]. However, compared with gradient descent, Sharpness-Aware Minimization is more often carried out under the framework of SGD optimizer. Under this setting, it is possible that the data (x_k, y_k) may not be used in some updating steps. Therefore, we utilize $B_{k,t}$ to indicate whether (x_k, y_k) is used in the t-th gradient descent step. Finally, we have the following result.

Theorem 4.6. *Assume the model is trained by SGD with the worst perturbation $\hat{\epsilon}(\cdot)$ in each iteration is calculated via (6). For the data (x_k, y_k), it Gradient trajectory-based IF (SAM-GIF) is defined as*

$$\textit{SAM-GIF}_{\textit{SGD}}(x_k,y_k)=\sum_{t=0}^{T-1}\eta_t B_{k,t}\nabla_\omega L_S^k(\omega_t+\hat{\epsilon}(\omega_t))$$

Then, the LOO retrained model ω_k under SAM can be estimated by

$$\omega_k\approx\omega^*-\textit{SAM-GIF}_{\textit{SGD}}(x_k,y_k).$$

4.3 Computation Acceleration and Practical Applications

4.3.1 Computation Acceleration

The SAM-HIF outlined in Section 4.1 requires calculations of the inverse Hessian-vector product (iHVP). To enhance the scalability of SAM-HIF, we will introduce one efficient acceleration technique to expedite the computation of iHVP.

Neumann Series Approximation Method. The calculation in Proposition 4.3 and Theorem 4.5 is expressed as $-H^{-1}\cdot G$, where H denotes the Hessian and G is the gradient. Then, with the help of the Neumann series:

$$H^{-1}\cdot G=\left(I-(I-H)\right)^{-1}\cdot G=G+\sum_{j=1}^{+\infty}(I-H)^j\cdot G.$$

By truncating this series at order J, we derive the following approximation:

$$H^{-1}\cdot G\approx G+(I-H)\cdot G+\cdots(I-H)^J\cdot G.$$

It is important to clarify that we did not specifically focus on accelerating the inversion of the Hessian matrix; instead, we optimized the iHVP process directly. This approach eliminates the need to store the large Hessian matrix during the computation, which significantly reduces the memory requirements of our method.

4.3.2 Practical Applications

This section presents several downstream tasks based on the previously derived SAM-HIF and SAM-GIF for different scenarios.

Model Editing. We can use IFs to update the model under the removal of certain data. Specifically, the model after removing the k-th data point can be estimated as $\omega^* - \text{SAM-HIF}(x_k, y_k; \omega^*)$. Additionally, if the training gradient trajectory is available, we can obtain an efficient and accurate estimate as $\omega^* - \text{SAM-GIF}(x_k, y_k; \omega^*)$.

Data Evaluation. By appropriately selecting the model evaluation function, we can define influence scores (ISs) for individual data points. These scores can then be applied to data selection to enhance SAM performance.

Definition 4.7. (Evaluation Function) Given a validation dataset defined as $D_{val} = \{(x_t, y_t)\}_{t=1}^n$. the SAM learned parameter ω^* performance on the test task is defined as $\sum_{(x,y)\in D_{val}} \ell(x, y; \omega^*)$.

Based on this metric, we can propose an evaluation method for the data influence.

Theorem 4.8. *Given a validation dataset defined as $D_{val} = \{(x_t, y_t)\}_{t=1}^n$. Denote the SAM-retrained model after the removal of (x_k, y_k) as ω^*_{-k}, then*

$$\begin{aligned} &\sum_{(x,y)\in D_{val}} \ell(x, y; \omega^*) - \sum_{(x,y)\in D_{val}} \ell(x, y; \omega^*_{-k}) \\ \approx &\sum_{(x,y)\in D_{val}} \nabla \ell(x, y; \omega^*) \cdot \mathit{IF}(x, y) \triangleq \mathit{IS}(x, y), \end{aligned}$$

where IF can be SAM-HIF or SAM-GIF. We define the right hand of the above equation as the Influence Score (IS).

A positive IS indicates that removing the data point will deteriorate the model's performance on the test dataset. Thus, this data point is valuable for model performance. Assigning an IS to each training data point allows us to identify useful and harmful data for the model's performance. Detailed theoretical derivations are provided in the Appendix.

5 Experiments

In this section, we demonstrate our main experimental results on utility, efficiency, effectiveness, and the abilities to identify harmful data and enhance interpretability. Details and additional results are in Appendix due to space limit.

5.1 Experimental Settings

Dataset. To evaluate the performance of our algorithm, we conducted experiments using four datasets: CIFAR10, CIFAR100 [1], MiniImageNet [13], MNIST [37], and HAM10000 [53]. MiniImageNet, a subset of the larger ImageNet dataset, is commonly employed in few-shot learning research due to its diverse class representations and moderate resolution.

Baselines. We employ retraining as the baseline method since the data valuation problem in SAM has never been investigated, and there are no other baselines. *Retrain*: We retrain the model via SAM after removing the data from the training set. In scenarios where the model training trajectory cannot be obtained, we employ SAM-HIF (fast) and SAM-HIF. *SAM-HIF (fast)*: SAM-HIF (fast) is a direct implementation of our previous Theorem 4.3. *SAM-HIF*: SAM-HIF is a direct implementation of our previous Theorem 4.5.

In scenarios where the model training trajectory is available, we employ SAM-GIF. *SAM-GIF*: SAM-GIF is a direct implementation of our previous Theorem 4.6. For the methods mentioned above, we provide corresponding algorithms in the Appendix. SAM-HIF (fast) and SAM-HIF are accelerated by the Neumann Series approximation method discussed in Section 4.3.1. We provide implementation algorithms for SAM-HIF (fast), SAM-HIF and SAM-GIF in the Appendix.

Evaluation Metric. We used two primary evaluation metrics to assess our models: accuracy and runtime (RT). Accuracy evaluates the model's performance by measuring the proportion of correctly classified instances out of the total instances. Runtime(RT), measured in seconds, assesses the time required for each method to update the model.

Implementation Details. We conducted experiments using the Nvidia RTX 4090-24G GPU. For utility evaluation, we randomly selected samples at different proportions from four datasets. For

valuable (or harmful) samples, we removed 0-10 % of the data identified as valuable (or harmful) by the algorithm. Additionally, the removal process was repeated five times using different random seeds to obtain experimental results.

5.2 Evaluation of Utility and Editing Efficiency

We first demonstrate the results on accuracy and time consumption of three algorithms, SAM-HIF (fast), SAM-HIF, and SAM-GIF, against the retrain method. We selected the WideResNets architecture as the backbone network for the classification task. Our experimental results are presented in Table 1. It is evident that our three proposed algorithms significantly improve computational efficiency without sacrificing accuracy. On the CIFAR-10 dataset, the time cost of retraining reached 3516.74, while our methods notably enhance computational efficiency, with SAM-HIF (fast), SAM-HIF, and SAM-GIF reducing the time to 11.0698, 41.4960, and 4.894 seconds, respectively. The accuracy differences between SAM-HIF (fast), SAM-HIF, and SAM-GIF compared to retrain are 0.0177, 0.0057, and 0.0003, respectively. These findings suggest that SAM-HIF (fast), SAM-HIF, and SAM-GIF can save substantial computational time required for retraining while achieving comparable accuracy.

Table 1: Performance comparison on CIFAR-10, CIFAR-100, and MINI-Imagenet.

Method	**Cifar10**		**Cifar100**		**MINI-Imagenet**	
	Accuracy	**RT (second)**	**Accuracy**	**RT (second)**	**Accuracy**	**RT (second)**
Retrain	0.9500±0.0061	3516.74±8.45	0.7890±0.0311	3244.24±2.18	0.6835±0.0460	682.56±7.91
SAM-HIF(Fast)	0.9323±0.0110	11.0698±3.41	0.7208±0.0142	13.0698±4.16	0.6478±0.0125	11.3218±2.43
SAM-HIF	0.9443±0.0121	41.4960±3.21	0.7213±0.0239	42.412±3.24	0.6516±0.0213	39.212±3.09
SAM-GIF	0.9497±0.0142	4.8942±1.42	0.7227±0.0469	6.8942±2.31	0.6446±0.0122	5.8942±1.122

Furthermore, we observe that by avoiding the computation of the Hessian matrix, SAM-GIF requires less time than both SAM-HIF (Fast) and SAM-HIF. Besides, SAM-GIF not only surpasses SAM-HIF and SAM-HIF (Fast) in speed but also achieves accuracy comparable to retraining. This corroborates our previous discussion: compared to the SAM model, gradient trajectories can more accurately reflect the training of the SAM model, leading to a more precise estimation result. By avoiding the computation of the Hessian matrix, SAM-GIF demonstrates better time efficiency than other methods while also showing improved accuracy on CIFAR-10. These findings indicate that utilizing gradient information effectively enhances both training efficiency and predictive accuracy. Moreover, we can see SAM-HIF achieves higher accuracy than SAM-HIF (Fast) by incorporating perturbation-related components into the Hessian matrix; however, this comes at the cost of a 2-3$\times$ increase in runtime. Mathematically, as we mentioned in Theorem 4.5, SAM-HIF further considers the change of perturbations due to the data removal. This can make it evaluate data influence more accurately but with additional computation time. Please refer to section C.1 for more results.

We also compare with several baselines. We choose two algorithms: TARK [46] and IF-EKFAC. The results are listed in Table 2. We tested it on the Cifar-10 dataset. We first trained the Wide-Resnet model for 60 epochs and obtained an accuracy of 0.8132. Then, we compute the scores for all the training data and retrain by removing the bottom 10% of the data. For SAM-GIF, we also use our algorithm to estimate the parameters.

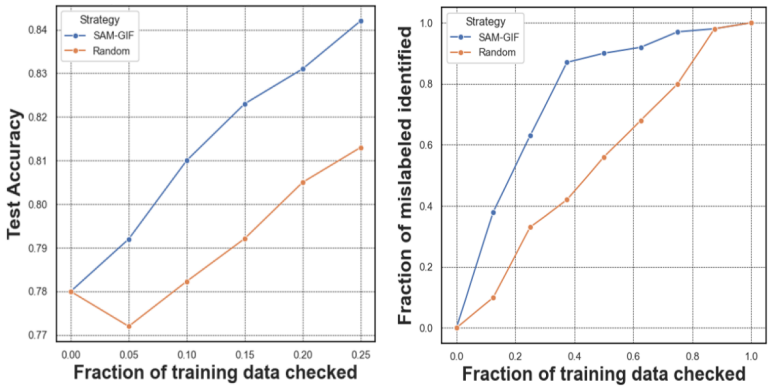
Table 2: Performance comparison of different methods on Cifar10 dataset.

Method	**Cifar10**	
	Accuracy	**RT (second)**
TARK	0.8321±0.0061	3314.23±10
IF-EKFAC	0.8323±0.0110	3338.94±10
SAM-GIF(Retrain)	0.8423±0.0142	3231.49±10
SAM-GIF(GIF)	0.8401±0.0142	5.1442±1.42

Furthermore, we perform experiments on Resnet-50 [23] and the results are shown in Table 3.

Table 3: Performance comparison on *Resnet50*.

Method	CUB		FOOD-101	
	Accuracy	RT (s)	Accuracy	RT (s)
Retrain	0.6336±0.005	2197.33±12.47	0.7436±0.031	15900.24±25.32
SAM-HIF	0.6213±0.005	37.2590±3.78	0.7022±0.024	41.321±4.12
SAM-HIF(Fast)	0.6178±0.003	25.3214±5.16	0.6918±0.014	26.0698±3.21
SAM-GIF	0.6244±0.004	12.6789±2.33	0.7189±0.047	13.234±3.23



(a) Test Accuracy (b) Harmful Data Removal

Figure 1: Harmful data removal experiment. IS means using the influence score to determine which sample to remove. Random refers to randomly removing tasks

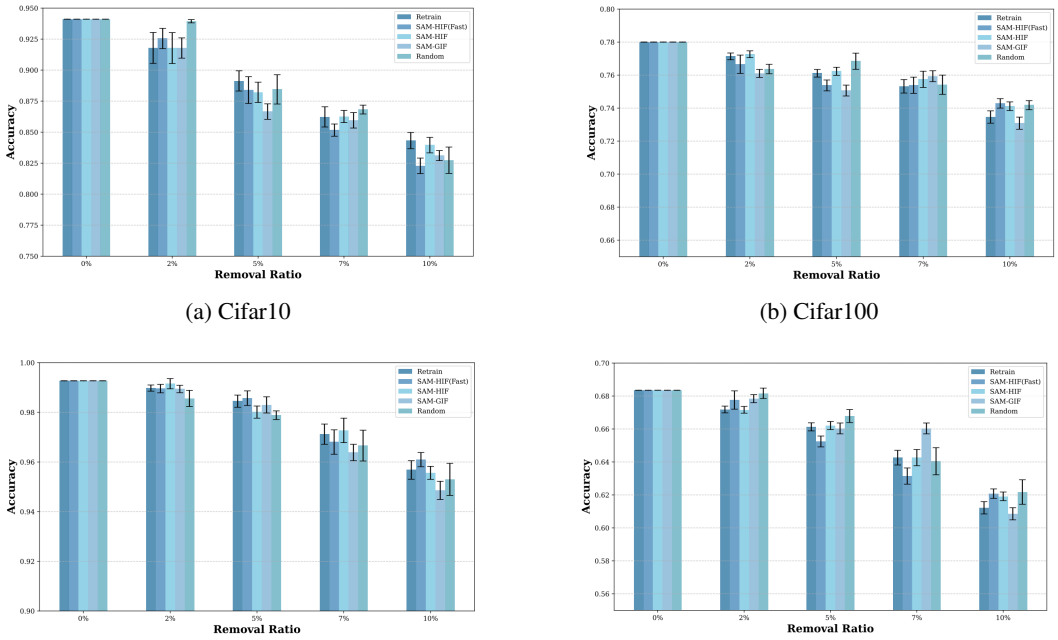
5.3 Evaluation of Effectiveness for Data Attribution

Here, we aim to show that our proposed influence functions can be used to attribute data. To achieve this, we traverse the training samples by calculating the IS value for each sample to select the most valuable data. We then remove these samples and update the model through retraining or using the SAM-HIF (Fast), SAM-HIF, and SAM-GIF, and analyzing the changes in accuracy relative to the accuracy before removal. In detail, we first calculate the influence scores of all samples and select the most valuable ones by ranking them. Then, the top k most valuable data points are removed, where k ranges from 2% to 10% of the data size. Next, the model is retrained multiple times using different random seeds or updated using our different methods. The test set accuracy is then calculated after updating the parameters. Additionally, we randomly delete the same proportion of samples as a control experiment.

Our experimental results, as shown in the Figure 2, indicate that after removing the most valuable training data, the accuracy of the updated model decreases across different datasets. For instance, for the CIFAR-10 dataset, when the removal ratios are 0.02, 0.05, 0.07, and 0.10, the accuracy scores for retraining and the SAM-HIF (Fast), SAM-HIF, and SAM-GIF algorithms gradually decrease. At the 0.10 removal ratio, the accuracy for the four methods drops to 0.8432, 0.8212, 0.8412, and 0.8311, respectively. The accuracy of different approaches is similar to that of retraining (with a maximum difference of 0.022), which demonstrates that our algorithm significantly reduces computational time while maintaining accuracy. In contrast, random deletion shows more significant variability, and while an increase in the deletion ratio may lead to an increase in accuracy, it is less stable.

5.4 Results of Identifying Harmful Data

To demonstrate the ability of our algorithm to identify harmful data for a specific task, we introduce noise into the CIFAR-10 dataset and conduct experiments on the noisy dataset. Specifically, we randomly select 10% of the CIFAR-10 data samples and invert their labels, then use the noisy dataset to train the model using the SAM method. The training setup remains consistent with previous configurations. We compute the IS of the samples using SAM-GIF, and then identify the data as harmful if its IS is low. We then compare the model accuracy after retraining with different proportions of harmful data points randomly removed. Figure 1a shows the change in model accuracy



(a) Cifar10 (b) Cifar100

(c) Mnist (d) Miniimagenet

Figure 2: Accuracy performance on four datasets after removing varying proportions of helpful data using task-related IS

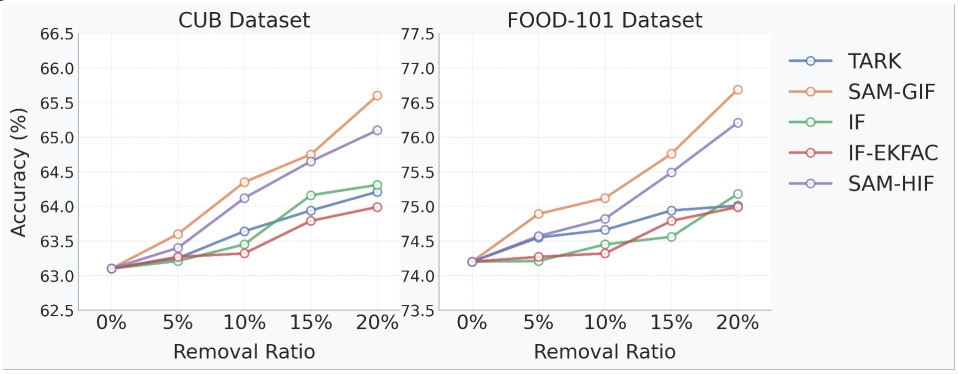


Figure 3: Harmful data removal results compared with baselines.

after removing varying proportions of harmful data, indicating that as the proportion of harmful data removed increases, the model's accuracy on the test set also improves. When the removal rate reaches 0.25, the accuracy increases by approximately 0.06. For random deletion, the accuracy exhibits considerable instability; initially, the accuracy decreases around a removal rate of 0.05, but it gradually increases as the removal rate increases. Figure 1b illustrates the proportion of noisy data detected after removing training samples. Compared to random deletion, our algorithm demonstrates higher efficiency in detecting noisy data. At a detection rate of approximately 0.4, we have identified over 90% of the noisy data. The experimental results for the remaining datasets can be found in the Appendix.

We also compare the performance of our method with TARK [46], Influence Function (IF), Influence Function-EKFAC (IF-EKFAC) in the harmful data recogonization task.

5.5 Results on Interpretability

We apply SAM-GIF to identify the training samples that are most relevant to specific prediction errors in the test samples. In this process, we select samples from the test data where the model misclassifies. By calculating the IS of the samples, we identify and visualize harmful data with a negative IS that leads to erroneous predictions, namely. Figure 4 presents the visualization of this error prediction

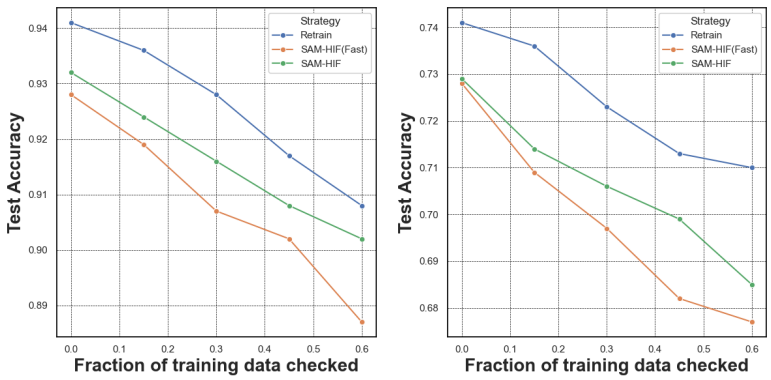


Figure 4: The most helpful and harmful training data tracked by misclassified data

tracing process for the CIFAR-10 dataset (more visualization results are in Appendix). The first row displays examples of misclassified test samples, the second row shows the most influential training data for classifying this sample, and the third row shows the most harmful training data for this classification. We can trace the outcomes of the error prediction process through the visualization results.

5.6 Ablation Study

We conducted ablation experiments on above three methods, SAM-HIF (fast), SAM-HIF and SAM-GIF. We randomly removed 1%-8% of the training samples from CIFAR-10 and CIFAR-100 datasets, and evaluated the model parameters using SAM-HIF(fast) and SAM-HIF, with retrain serving as the ground truth. The results, shown in Figure 5, clearly demonstrate that SAM-HIF consistently outperforms SAM-HIF(Fast) during the process of data removal. Also, we can see both methods consistently have slight differences with the ground truth. Results for SAM-GIF are included in the Appendix.



(a) CIFAR-10 (b) CIFAR-100

Figure 5: Ablation studies on CIFAR-10 and CIFAR-100.

6 Conclusion

In conclusion, we addressed data attribution challenges in the SAM framework with two novel methods: SAM-HIF and SAM-GIF. SAM-HIF employs a comprehensive closed-form data influence estimation. SAM-GIF utilizes gradient trajectory information for efficient, scalable evaluation. Experiments on four datasets demonstrated the effectiveness and scalability of these methods. Our approach aids in mislabeled data detection, model editing, and interpretability in SAM-trained models.

References

[1] Krizhevsky Alex. Learning multiple layers of features from tiny images. *https://www. cs. toronto. edu/kriz/learning-features-2009-TR. pdf*, 2009.

[2] Maksym Andriushchenko, Dara Bahri, Hossein Mobahi, and Nicolas Flammarion. Sharpness-aware minimization leads to low-rank features. *Advances in Neural Information Processing Systems*, 36:47032–47051, 2023.

[3] Maksym Andriushchenko and Nicolas Flammarion. Towards understanding sharpness-aware minimization. In *International Conference on Machine Learning*, pages 639–668. PMLR, 2022.

[4] Dara Bahri, Hossein Mobahi, and Yi Tay. Sharpness-aware minimization improves language model generalization. *arXiv preprint arXiv:2110.08529*, 2021.

[5] S Basu, P Pope, and S Feizi. Influence functions in deep learning are fragile. In *International Conference on Learning Representations (ICLR)*, 2021.

[6] Marc-Etienne Brunet, Colleen Alkalay-Houlihan, Ashton Anderson, and Richard Zemel. Understanding the origins of bias in word embeddings. In *International conference on machine learning*, pages 803–811. PMLR, 2019.

[7] Pratik Chaudhari, Anna Choromanska, Stefano Soatto, Yann LeCun, Carlo Baldassi, Christian Borgs, Jennifer Chayes, Levent Sagun, and Riccardo Zecchina. Entropy-sgd: Biasing gradient descent into wide valleys. *Journal of Statistical Mechanics: Theory and Experiment*, 2019(12):124018, 2019.

[8] Hongge Chen, Si Si, Yang Li, Ciprian Chelba, Sanjiv Kumar, Duane Boning, and Cho-Jui Hsieh. Multi-stage influence function. *Advances in Neural Information Processing Systems*, 33:12732–12742, 2020.

[9] Xiangning Chen, Cho-Jui Hsieh, and Boqing Gong. When vision transformers outperform resnets without pre-training or strong data augmentations. *arXiv preprint arXiv:2106.01548*, 2021.

[10] R Dennis Cook. Detection of influential observation in linear regression. *Technometrics*, 42(1):65–68, 2000.

[11] R Dennis Cook and Sanford Weisberg. Characterizations of an empirical influence function for detecting influential cases in regression. *Technometrics*, 22(4):495–508, 1980.

[12] John M Danskin. *The theory of max-min and its application to weapons allocation problems*, volume 5. Springer Science & Business Media, 2012.

[13] Jia Deng, Wei Dong, Richard Socher, Li-Jia Li, Kai Li, and Li Fei-Fei. Imagenet: A large-scale hierarchical image database. In *2009 IEEE Conference on Computer Vision and Pattern Recognition*, pages 248–255, 2009.

[14] Jiawei Du, Hanshu Yan, Jiashi Feng, Joey Tianyi Zhou, Liangli Zhen, Rick Siow Mong Goh, and Vincent YF Tan. Efficient sharpness-aware minimization for improved training of neural networks. *arXiv preprint arXiv:2110.03141*, 2021.

[15] Vitaly Feldman and Chiyuan Zhang. What neural networks memorize and why: Discovering the long tail via influence estimation. *Advances in Neural Information Processing Systems*, 33:2881–2891, 2020.

[16] Pierre Foret, Ariel Kleiner, Hossein Mobahi, and Behnam Neyshabur. Sharpness-aware minimization for efficiently improving generalization. *arXiv preprint arXiv:2010.01412*, 2020.

[17] Shaopeng Fu, Liang Ding, and Di Wang. " short-length" adversarial training helps llms defend" long-length" jailbreak attacks: Theoretical and empirical evidence. *arXiv preprint arXiv:2502.04204*, 2025.

[18] Shaopeng Fu and Di Wang. Theoretical analysis of robust overfitting for wide dnns: An ntk approach. *arXiv preprint arXiv:2310.06112*, 2023.

[19] Amirata Ghorbani and James Zou. Data shapley: Equitable valuation of data for machine learning. In *International conference on machine learning*, pages 2242–2251. PMLR, 2019.

[20] Aditya Golatkar, Alessandro Achille, Avinash Ravichandran, Marzia Polito, and Stefano Soatto. Mixed-privacy forgetting in deep networks. In *Proceedings of the IEEE/CVF conference on computer vision and pattern recognition*, pages 792–801, 2021.

[21] Aditya Golatkar, Alessandro Achille, and Stefano Soatto. Eternal sunshine of the spotless net: Selective forgetting in deep networks. In *Proceedings of the IEEE/CVF Conference on Computer Vision and Pattern Recognition*, pages 9304–9312, 2020.

[22] Xiaochuang Han, Byron C Wallace, and Yulia Tsvetkov. Explaining black box predictions and unveiling data artifacts through influence functions. *arXiv preprint arXiv:2005.06676*, 2020.

[23] Kaiming He, Xiangyu Zhang, Shaoqing Ren, and Jian Sun. Deep residual learning for image recognition. In *Proceedings of the IEEE conference on computer vision and pattern recognition*, pages 770–778, 2016.

[24] Sepp Hochreiter and Jürgen Schmidhuber. Simplifying neural nets by discovering flat minima. *Advances in neural information processing systems*, 7, 1994.

[25] Sepp Hochreiter and Jürgen Schmidhuber. Flat minima. *Neural computation*, 9(1):1–42, 1997.

[26] Lijie Hu, Ivan Habernal, Lei Shen, and Di Wang. Differentially private natural language models: Recent advances and future directions. *arXiv preprint arXiv:2301.09112*, 2023.

[27] Lijie Hu, Chenyang Ren, Zhengyu Hu, Hongbin Lin, Cheng-Long Wang, Hui Xiong, Jingfeng Zhang, and Di Wang. Editable concept bottleneck models. *arXiv preprint arXiv:2405.15476*, 2024.

[28] Lijie Hu, Chenyang Ren, Huanyi Xie, Khouloud Saadi, Shu Yang, Zhen Tan, Jingfeng Zhang, and Di Wang. Dissecting representation misalignment in contrastive learning via influence function. *arXiv preprint arXiv:2411.11667*, 2024.

[29] Lijie Hu, Zihang Xiang, Jiabin Liu, and Di Wang. Privacy-preserving sparse generalized eigenvalue problem. In *International Conference on Artificial Intelligence and Statistics*, pages 5052–5062. PMLR, 2023.

[30] Peter J Huber. Robust statistics. *Wiley Series in Probability and Mathematical Statistics*, 1981.

[31] Pavel Izmailov, Dmitrii Podoprikhin, Timur Garipov, Dmitry Vetrov, and Andrew Gordon Wilson. Averaging weights leads to wider optima and better generalization. *arXiv preprint arXiv:1803.05407*, 2018.

[32] Ruoxi Jia, David Dao, Boxin Wang, Frances Ann Hubis, Nick Hynes, Nezihe Merve Gürel, Bo Li, Ce Zhang, Dawn Song, and Costas J Spanos. Towards efficient data valuation based on the shapley value. In *The 22nd International Conference on Artificial Intelligence and Statistics*, pages 1167–1176. PMLR, 2019.

[33] Nitish Shirish Keskar, Dheevatsa Mudigere, Jorge Nocedal, Mikhail Smelyanskiy, and Ping Tak Peter Tang. On large-batch training for deep learning: Generalization gap and sharp minima. *arXiv preprint arXiv:1609.04836*, 2016.

[34] Pang Wei Koh and Percy Liang. Understanding black-box predictions via influence functions. In *International conference on machine learning*, pages 1885–1894. PMLR, 2017.

[35] Jungmin Kwon, Jeongseop Kim, Hyunseo Park, and In Kwon Choi. Asam: Adaptive sharpness-aware minimization for scale-invariant learning of deep neural networks. In *International Conference on Machine Learning*, pages 5905–5914. PMLR, 2021.

[36] Yongchan Kwon and James Zou. Beta shapley: a unified and noise-reduced data valuation framework for machine learning. In *Proceedings of The 25th International Conference on Artificial Intelligence and Statistics*, 2022.

[37] Yann LeCun, Léon Bottou, Yoshua Bengio, and Patrick Haffner. Gradient-based learning applied to document recognition. *Proceedings of the IEEE*, 86(11):2278–2324, 1998.

[38] Guanghua Liu, Jia Zhang, Peng Lv, Chenlong Wang, Huan Wang, and Di Wang. Taad: Time-varying adversarial anomaly detection in dynamic graphs. *Information Processing & Management*, 62(1):103912, 2025.

[39] Jiaqi Liu, Jian Lou, Zhan Qin, and Kui Ren. Certified minimax unlearning with generalization rates and deletion capacity. *Advances in Neural Information Processing Systems*, 36, 2024.

[40] Jinxin Liu and Zao Yang. Tracing privacy leakage of language models to training data via adjusted influence functions. *arXiv preprint arXiv:2408.10468*, 2024.

[41] Yong Liu, Siqi Mai, Xiangning Chen, Cho-Jui Hsieh, and Yang You. Towards efficient and scalable sharpness-aware minimization. In *Proceedings of the IEEE/CVF Conference on Computer Vision and Pattern Recognition*, pages 12360–12370, 2022.

[42] Scott Lundberg. A unified approach to interpreting model predictions. *arXiv preprint arXiv:1705.07874*, 2017.

[43] Zihao Luo, Xilie Xu, Feng Liu, Yun Sing Koh, Di Wang, and Jingfeng Zhang. Privacy-preserving low-rank adaptation against membership inference attacks for latent diffusion models. In *Proceedings of the AAAI Conference on Artificial Intelligence*, volume 39(6), pages 5883–5891, 2025.

[44] Aleksander Mądry, Aleksandar Makelov, Ludwig Schmidt, Dimitris Tsipras, and Adrian Vladu. Towards deep learning models resistant to adversarial attacks. *stat*, 1050(9), 2017.

[45] Behnam Neyshabur, Srinadh Bhojanapalli, David McAllester, and Nati Srebro. Exploring generalization in deep learning. *Advances in neural information processing systems*, 30, 2017.

[46] Sung Min Park, Kristian Georgiev, Andrew Ilyas, Guillaume Leclerc, and Aleksander Madry. Trak: Attributing model behavior at scale. *arXiv preprint arXiv:2303.14186*, 2023.

[47] Garima Pruthi, Frederick Liu, Satyen Kale, and Mukund Sundararajan. Estimating training data influence by tracing gradient descent. *Advances in Neural Information Processing Systems*, 33:19920–19930, 2020.

[48] Zhe Qu, Xingyu Li, Rui Duan, Yao Liu, Bo Tang, and Zhuo Lu. Generalized federated learning via sharpness aware minimization. In *International conference on machine learning*, pages 18250–18280. PMLR, 2022.

[49] Chenyang Ren, Huanyi Xie, Shu Yang, Meng Ding, Lijie Hu, and Di Wang. Evaluating data influence in meta learning. *arXiv preprint arXiv:2501.15963*, 2025.

[50] Marco Tulio Ribeiro, Sameer Singh, and Carlos Guestrin. " why should i trust you?" explaining the predictions of any classifier. In *Proceedings of the 22nd ACM SIGKDD international conference on knowledge discovery and data mining*, pages 1135–1144, 2016.

[51] Andrea Schioppa, Katja Filippova, Ivan Titov, and Polina Zablotskaia. Theoretical and practical perspectives on what influence functions do. *Advances in Neural Information Processing Systems*, 36, 2024.

[52] Ali Shafahi, Mahyar Najibi, Mohammad Amin Ghiasi, Zheng Xu, John Dickerson, Christoph Studer, Larry S Davis, Gavin Taylor, and Tom Goldstein. Adversarial training for free! *Advances in neural information processing systems*, 32, 2019.

[53] Philipp Tschandl, Cliff Rosendahl, and Harald Kittler. The ham10000 dataset, a large collection of multi-source dermatoscopic images of common pigmented skin lesions. *Scientific data*, 5(1):1–9, 2018.

[54] Di Wang, Lijie Hu, Huanyu Zhang, Marco Gaboardi, and Jinhui Xu. Generalized linear models in non-interactive local differential privacy with public data. *Journal of Machine Learning Research*, 24(132):1–57, 2023.

[55] Hao Wang, Berk Ustun, and Flavio Calmon. Repairing without retraining: Avoiding disparate impact with counterfactual distributions. In *International Conference on Machine Learning*, pages 6618–6627. PMLR, 2019.

[56] Eyal Winter. The shapley value. *Handbook of game theory with economic applications*, 3:2025–2054, 2002.

[57] Lijun Wu, Juntao Li, Yue Wang, Qi Meng, Tao Qin, Wei Chen, Min Zhang, Tie-Yan Liu, et al. R-drop: Regularized dropout for neural networks. *Advances in Neural Information Processing Systems*, 34:10890–10905, 2021.

[58] Mengzhou Xia, Sadhika Malladi, Suchin Gururangan, Sanjeev Arora, and Danqi Chen. Less: Selecting influential data for targeted instruction tuning. *arXiv preprint arXiv:2402.04333*, 2024.

[59] Zihang Xiang, Tianhao Wang, Wanyu Lin, and Di Wang. Practical differentially private and byzantine-resilient federated learning. *Proceedings of the ACM on Management of Data*, 1(2):1–26, 2023.

[60] Zihang Xiang, Tianhao Wang, and Di Wang. Preserving node-level privacy in graph neural networks. In *2024 IEEE Symposium on Security and Privacy (SP)*, pages 4714–4732. IEEE, 2024.

[61] Hanshen Xiao, Zihang Xiang, Di Wang, and Srinivas Devadas. A theory to instruct differentially-private learning via clipping bias reduction. In *2023 IEEE Symposium on Security and Privacy (SP)*, pages 2170–2189. IEEE, 2023.

[62] Jinsung Yoon, Sercan Arik, and Tomas Pfister. Data valuation using reinforcement learning. In *International Conference on Machine Learning*, pages 10842–10851. PMLR, 2020.

[63] Yuichi Yoshida and Takeru Miyato. Spectral norm regularization for improving the generalizability of deep learning. *arXiv preprint arXiv:1705.10941*, 2017.

[64] Jiaming Zhang, Mingxi Lei, Meng Ding, Mengdi Li, Zihang Xiang, Difei Xu, Jinhui Xu, and Di Wang. Towards user-level private reinforcement learning with human feedback. *arXiv preprint arXiv:2502.17515*, 2025.

[65] Lin Zhang, Lijie Hu, and Di Wang. Mechanistic unveiling of transformer circuits: Self-influence as a key to model reasoning. *arXiv preprint arXiv:2502.09022*, 2025.

[66] Ruijia Zhang, Mingxi Lei, Meng Ding, Zihang Xiang, Jinhui Xu, and Di Wang. Improved rates of differentially private nonconvex-strongly-concave minimax optimization. In *Proceedings of the AAAI Conference on Artificial Intelligence*, volume 39(21), pages 22524–22532, 2025.

[67] Yang Zhao, Hao Zhang, and Xiuyuan Hu. Penalizing gradient norm for efficiently improving generalization in deep learning. In *International Conference on Machine Learning*, pages 26982–26992. PMLR, 2022.

[68] Tianhang Zheng, D Wang, Baochun Li, and Jinhui Xu. Towards assessment of randomized mechanisms for certifying adversarial robustness. *arXiv preprint arXiv:2005.07347*, 2020.

A Omitted Proofs

A.1 Evaluating Data Attribution in SAM via Hessian-based IF

Theorem A.1. *Consider the data (x_k, y_k) along with a SAM-trained model ω^*, $\hat{\epsilon}(\omega^*)$ represents the model weight perturbation that results in the largest loss. Then the corresponding SAM-IF is defined as:*

$$\textit{SAM-IF}(x_k, y_k) = -H_\omega^{-1} \cdot \nabla L_S^k(\omega^* + \hat{\epsilon}(\omega^*))$$

where H_ω is defined as $H_\omega = \nabla^2 L_S\left(\omega^* + \hat{\epsilon}(\omega^*)\right) + \lambda \cdot I$. ω_k can be approximated by

$$\omega_k \approx \omega^* - \textit{SAM-IF}(x_k, y_k).$$

Proof. Recalling the definition $\hat{\epsilon}(\omega) = \arg\max_{||\epsilon||_p \leq \rho} L_S(\omega + \epsilon)$ and

$$\begin{aligned}
\omega^* &= \arg\min_\omega L_S(\omega) + \frac{\lambda}{2} \cdot ||\omega||_2^2 \\
&= \arg\min_\omega L_S(\omega + \hat{\epsilon}(\omega)) + \frac{\lambda}{2} \cdot ||\omega||_2^2 \\
&= \arg\min_\omega \sum_{i=1}^n \ell(x_i, y_i; \omega + \hat{\epsilon}(\omega)) + \frac{\lambda}{2} \cdot ||\omega||_2^2 \\
&= \arg\min_\omega \sum_{i=1}^n L_S^i(\omega + \hat{\epsilon}(\omega)) + \frac{\lambda}{2} \cdot ||\omega||_2^2
\end{aligned} \tag{8}$$

Now we consider removing the k-th data (x_k, y_k). The retrained parameter after the removal is denoted as ω_k:

$$\omega_k = \arg\min_\omega \sum_{i=1, i\neq k}^n L_S^i(\omega + \hat{\epsilon}(\omega)) + \frac{\lambda}{2} \cdot ||\omega||_2^2$$

To estimate this ω_k, we can firstly up-weigh the loss term $L_S^k(\omega + \hat{\epsilon}(\omega))$ by δ in the original loss function defined in (8), then a series of optimization problem can be defined as:

$$\omega_\delta = \arg\min_\omega L_S(\omega + \hat{\epsilon}_\delta(\omega)) + \delta \cdot L_S^k(\omega + \hat{\epsilon}_\delta(\omega)) + \frac{\lambda}{2} \cdot ||\omega||_2^2 \tag{9}$$

Noting here $\hat{\epsilon}_\delta(\omega)$ will change according to δ and is defined as

$$\hat{\epsilon}_\delta(\omega) = \arg\max_{||\epsilon||_p \leq \rho} \left[L_S(\omega + \epsilon) + \delta \cdot L_S^k(\omega + \epsilon)\right]$$

From the minimizing condition in Equation (8) and (9) and Lemma 4.2, we have

$$\nabla L_S(\omega^* + \hat{\epsilon}(\omega^*)) = 0, \nabla L_S(\omega_\delta + \hat{\epsilon}_\delta(\omega_\delta)) + \delta \cdot \nabla L_S^k(\omega_\delta + \hat{\epsilon}_\delta(\omega_\delta)) = 0. \tag{10}$$

To estimate $\omega_\delta - \omega^*$, we perform a Taylor expand at ω^* for the first equation in (10).:

$$\begin{aligned}
0 = &\nabla L_S\left(\omega^* + \hat{\epsilon}(\omega^*)\right) + \delta \cdot \nabla L_S^k\left(\omega^* + \hat{\epsilon}(\omega^*)\right) + \nabla^2 L_S\left(\omega^* + \hat{\epsilon}(\omega^*)\right) \cdot (\omega_\delta - \omega^*) \\
&+ \nabla^2 L_S\left(\omega^* + \hat{\epsilon}(\omega^*)\right) \cdot \left(\hat{\epsilon}_\delta\left(\omega_\delta\right) - \hat{\epsilon}(\omega^*)\right)
\end{aligned} \tag{11}$$

In the above expansion, the first term equals 0 from (10). And to make thing easier, we can neglect the last term and deduce a simple influence function for SAM.

$$\text{SAM-IF}(x_k, y_k) = \left.\frac{\mathrm{d}\omega_\delta}{\mathrm{d}\delta}\right|_{\delta=0} = -H_\omega^{-1} \cdot \nabla L_S^k(\omega^* + \hat{\epsilon}(\omega^*)),$$

where H_ω is defined as $H_\omega = \nabla^2 L_S\left(\omega^* + \hat{\epsilon}(\omega^*)\right) + \lambda \cdot I$.

When $\delta = -1$, ω_δ becomes ω_k. Then ω_k can be approximated by a first-order Taylor expansion:

$$\omega_k \approx \omega^* - \text{SAM-IF}(x_k, y_k).$$

□

Lemma A.2. *The term $\hat{\epsilon}_{k,\delta}\left(\omega_{k,\delta}\right)-\hat{\epsilon}(\omega^*)$ can be approximated by*

$$\begin{aligned}&\hat{\epsilon}_{k,\delta}(\omega_{k,\delta})-\hat{\epsilon}(\omega^*)\\=&\hat{\epsilon}_{k,\delta}(\omega^*)-\hat{\epsilon}(\omega^*)+\left.\frac{\mathrm{d}\hat{\epsilon}_{k,\delta}(\omega)}{\mathrm{d}\omega}\right|_{\omega=\omega^*}\cdot(\omega_{k,\delta}-\omega^*).\end{aligned}\tag{12}$$

Proof. Now, we begin to estimate $\hat{\epsilon}_{k,\delta}(\omega_{k,\delta})-\hat{\epsilon}(\omega^*)$. Recalling the definitions as following:

$$\begin{aligned}\hat{\epsilon}_{k,\delta}\left(\omega_{k,\delta}\right)&=\underset{||\epsilon||_p\leq\rho}{\arg\max}\left[L_S(\omega_{k,\delta}+\epsilon)+\delta\cdot L_S^k(\omega_{k,\delta}+\epsilon)\right],\\\hat{\epsilon}(\omega^*)&=\underset{||\epsilon||_p\leq\rho}{\arg\max}.L_S(\omega^*+\epsilon)\end{aligned}$$

We will use $\hat{\epsilon}_{k,\delta}(\omega^*)$ as an intermediate variable to simplify the approximation, which is defined as

$$\hat{\epsilon}_{k,\delta}(\omega^*)=\underset{||\epsilon||_p\leq\rho}{\arg\min}\left[L_S(\omega^*+\epsilon)+\delta\cdot L_S^k(\omega^*+\epsilon)\right]$$

Firstly, we perform a Taylor expansion for $\hat{\epsilon}_{k,\delta}\left(\omega_{k,\delta}\right)$ at ω^* as follows:

$$\hat{\epsilon}_{k,\delta}\left(\omega_{k,\delta}\right)\approx\hat{\epsilon}_{k,\delta}\left(\omega^*\right)+\left.\frac{\mathrm{d}\hat{\epsilon}_{k,\delta}\left(\omega_{k,\delta}\right)}{\mathrm{d}\omega}\right|_{\omega=\omega^*}\cdot\left(\omega_{k,\delta}-\omega^*\right)$$

Then the objective to estimate becomes

$$\begin{aligned}&\hat{\epsilon}_{k,\delta}(\omega_{k,\delta})-\hat{\epsilon}(\omega^*)\\=&\hat{\epsilon}_{k,\delta}(\omega_{k,\delta})-\hat{\epsilon}_{k,\delta}(\omega^*)+\hat{\epsilon}_{k,\delta}(\omega^*)-\hat{\epsilon}(\omega^*)\\=&\hat{\epsilon}_{k,\delta}(\omega^*)-\hat{\epsilon}(\omega^*)+\left.\frac{\mathrm{d}\hat{\epsilon}_{k,\delta}\left(\omega_{k,\delta}\right)}{\mathrm{d}\omega}\right|_{\omega=\omega^*}\cdot\left(\omega_{k,\delta}-\omega^*\right)\end{aligned}$$

□

Theorem A.3. *Consider the k-th data (x_k,y_k) along with a SAM-trained model ω^*. Define the Hessian-based influence function for SAM(SAM-HIF) as:*

$$\begin{aligned}&\textit{SAM-HIF}(x_k,y_k)\\=&-\left(H_\omega+H_\omega\cdot\frac{\mathrm{d}\hat{\epsilon}(\omega^*)}{\mathrm{d}\omega}\right)^{-1}\cdot\nabla L_S^k\left(\omega^*+\hat{\epsilon}(\omega^*)\right).\end{aligned}$$

Then ω_k can be approximated by:

$$\omega_k\approx\omega^*-\textit{SAM-HIF}(x_k,y_k).$$

Proof. Based on the expansion in Equation (11) in Theorem A.1, we can further estimate the term $\hat{\epsilon}_{k,\delta}\left(\omega_{k,\delta}\right)-\hat{\epsilon}(\omega^*)$ by Lemma 5:

$$\begin{aligned}0=&\nabla L_S\left(\omega^*+\hat{\epsilon}(\omega^*)\right)+\delta\cdot\nabla L_S^k\left(\omega^*+\hat{\epsilon}(\omega^*)\right)+\nabla^2L_S\left(\omega^*+\hat{\epsilon}(\omega^*)\right)\cdot(\omega_\delta-\omega^*)\\&+\nabla^2L_S\left(\omega^*+\hat{\epsilon}(\omega^*)\right)\cdot\left(\hat{\epsilon}_\delta(\omega^*)-\hat{\epsilon}(\omega^*)+\left.\frac{\mathrm{d}\hat{\epsilon}_\delta\left(\omega_\delta\right)}{\mathrm{d}\omega}\right|_{\omega=\omega^*}\cdot\left(\omega_\delta-\omega^*\right)\right)\end{aligned}\tag{13}$$

The first term equals 0 from (10). Then we have

$$0=\delta\cdot\nabla L_S^k\left(\omega^*+\hat{\epsilon}(\omega^*)\right)+\left(H_\omega+H_\omega\cdot\frac{\mathrm{d}\hat{\epsilon}_\delta\left(\omega_\delta\right)}{\mathrm{d}\omega}\right)\cdot(\omega_\delta-\omega^*)+H_\omega\cdot\left(\hat{\epsilon}_\delta(\omega^*)-\hat{\epsilon}(\omega^*)\right).\tag{14}$$

Then

$$\begin{aligned}\omega_\delta-\omega^*=&-\left(H_\omega+H_\omega\cdot\frac{\mathrm{d}\hat{\epsilon}_\delta\left(\omega_\delta\right)}{\mathrm{d}\omega}\right)^{-1}\cdot H_\omega\cdot\left(\hat{\epsilon}_\delta(\omega^*)-\hat{\epsilon}(\omega^*)\right)\\&-\delta\cdot\left(H_\omega+H_\omega\cdot\frac{\mathrm{d}\hat{\epsilon}_\delta\left(\omega_\delta\right)}{\mathrm{d}\omega}\right)^{-1}\cdot\nabla L_S^k\left(\omega^*+\hat{\epsilon}(\omega^*)\right).\end{aligned}$$

Then we can obtain the following equation:

$$\begin{aligned}\left.\frac{\mathrm{d}\omega_\delta}{\mathrm{d}\delta}\right|_{\delta=0} = &-\left(H_\omega + H_\omega \cdot \frac{\mathrm{d}\hat{\epsilon}\left(\omega^*\right)}{\mathrm{d}\omega}\right)^{-1} \cdot H_\omega \cdot \left.\frac{\mathrm{d}\hat{\epsilon}_\delta(\omega^*)}{\mathrm{d}\delta}\right|_{\delta=0} \\ &-\left(H_\omega + H_\omega \cdot \frac{\mathrm{d}\hat{\epsilon}\left(\omega^*\right)}{\mathrm{d}\omega}\right)^{-1} \cdot \nabla L_S^k\left(\omega^* + \hat{\epsilon}(\omega^*)\right).\end{aligned}$$

To enhance the computation efficiency, we drop the first term, and obtain the SAM-HIF as

$$\text{SAM-IF} = \left.\frac{\mathrm{d}\omega_\delta}{\mathrm{d}\delta}\right|_{\delta=0} = -\left(H_\omega + H_\omega \cdot \frac{\mathrm{d}\hat{\epsilon}\left(\omega^*\right)}{\mathrm{d}\omega}\right)^{-1} \cdot \nabla L_S^k\left(\omega^* + \hat{\epsilon}(\omega^*)\right). \tag{15}$$

□

A.2 Computation Acceleration

Theorem A.4. *Given a validation dataset defined as $D_{val} = \{(x_t, y_t)\}_{t=1}^n$. Denote the SAM-retrained model after the removal of (x_k, y_k) as ω_{-k}^*, then*

$$\begin{aligned}&\sum_{(x,y)\in D_{val}} \ell(x, y; \omega^*) - \sum_{(x,y)\in D_{val}} \ell(x, y; \omega_{-k}^*) \\ \approx &\sum_{(x,y)\in D_{val}} \nabla\ell(x, y; \omega^*) \cdot \mathit{IF}(x, y) \triangleq \mathit{IS}(x, y),\end{aligned}$$

where IF can be SAM-HIF or SAM-GIF. We define the right hand of the above equation as the Influence Score (IS).

Proof.

$$\begin{aligned}&\sum_{(x,y)\in D_{val}} \ell(x, y; \omega^*) - \sum_{(x,y)\in D_{val}} \ell(x, y; \omega_{-k}^*) \\ \approx &\sum_{(x,y)\in D_{val}} \nabla\ell(x, y; \omega^*) \cdot \left(\omega^* - \omega_{-k}^*\right) \\ = &\sum_{(x,y)\in D_{val}} \nabla\ell(x, y; \omega^*) \cdot \mathrm{IF}(x, y) \triangleq \mathrm{IS}(x, y).\end{aligned}$$

□

B Omitted Algorithms

Algorithm 2 SAM-IF with gradient trajectory

1: **Input:**
data: Training Dataset $S = \{(x_i, y_i\}_{i=1}^n$, data point (x_k, y_k) to be evaluated.
Parameter: Parameter checkpoint set $\Omega = \{\omega_c\}_{c=1}^s$, learning rate η_c at step c.

2: Compute the influence of (x_k, y_k) in the c-th checkpoint as

$$\text{IF}_c = \eta_c \cdot \nabla L_S^k(\omega_{c-1} + \hat{\epsilon}(\omega_{c-1}))$$

3: Sum up to obtain the final influence as

$$\text{SAM-IF}_{\text{Step}} = \sum_{c=1}^{s} \text{IF}_c$$

4: **Return:** SAM-IF$_{\text{Step}}$. Final Parameter $\omega^- = \omega^* -$ SAM-IF.

Algorithm 3 Simple SAM-IF

1: **Input:**
Data: Training Dataset $S = \{(x_i, y_i\}_{i=1}^n$, data point (x_k, y_k) to be evaluated.
Parameter: The learned SAM-parameter ω^*, the learned best perturbation $\hat{\epsilon}$.

2: Compute T^k as:

$$T^k = \nabla L_S^k \left(\omega^* + \hat{\epsilon}\right)$$

3: Define the Hessian matrix H as:

$$\nabla^2 L_S \left(\omega^* + \hat{\epsilon}\right)$$

4: Use EK-FAC to compute the Hessian-vector product of H and T^k:

$$\text{SAM-IF} = -H^{-1} \cdot T^k$$

5: Obtain the estimated parameter by

$$\omega^- = \omega^* - \text{SAM-IF}.$$

6: **Return:** SAM-IF, ω^-.

Algorithm 4 SAM-IF with total Hessian

Input:
Data: Training Dataset $S = \{(x_i, y_i\}_{i=1}^n$, data point (x_k, y_k) to be evaluated.
Parameter: The learned SAM-parameter ω^*, the learned best perturbation $\hat{\epsilon}$.
Compute T^k as:

$$T^k = \nabla L_S^k \left(\omega^* + \hat{\epsilon}\right)$$

Define the gradient of ϵ as

$$C^\epsilon = \nabla_\omega \frac{|\nabla_w L_S(\omega^*)|^{q-1}}{\left(\|\nabla_w L_S(\omega^*)\|_q^q\right)^{1/p}}$$

Give the definition of H as

$$H = \nabla^2 L_S \left(\omega^* + \hat{\epsilon}\right) + \nabla^2 L_S \left(\omega^* + \hat{\epsilon}\right) \cdot C^\epsilon.$$

$j \leftarrow 1$
$T^k \leftarrow I_0$
if $\|I_j - I_{j-1}\|_1 > \zeta$ **then**
    Use EK-FAC to compute the Hessian-vector product $S_j \triangleq H \cdot I_j$.
    Compute I_{j+1} by

$$I_{j+1} = I_j - \delta \cdot I_j + S_j + T^k$$

    $j \leftarrow j + 1$
end if
SAM-IF $\leftarrow I_{j+1}$.
Obtain the estimated parameter by $\omega^- = \omega^* -$ SAM-IF.
Return: SAM-IF. ω^-.

C Additional Experiment Results

This section presents the additional experimental results for completeness and detailed analysis.

C.1 Results of Efficiency and Accuracy

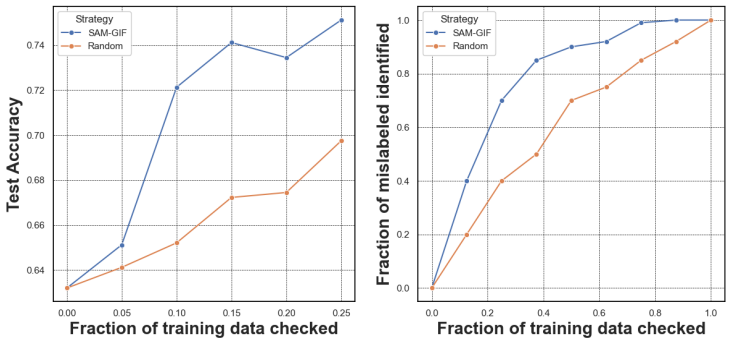
We conduct experiments on MNIST and HAM with Wide-Resnet as the model.

Table 4: Performance comparison on MNIST and HAM.

Method	Mnist		HAM	
	Accuracy	RT (second)	Accuracy	RT (second)
Retrain	0.9927±0.0005	2304.24±7.91	0.7254±0.02	2300.00±10.00
SAM-HIF(Fast)	0.9876±0.0013	8.0698±2.91	0.7130±0.0150	15.00±2.00
SAM-HIF	0.9880±0.0011	18.2321±1.91	0.7212±0.0120	52.20±3.00
SAM-GIF	0.9884±0.0007	2.8212±1.91	0.7350±0.0110	4.320±1.50

C.2 Results of Identifying Harmful Data

We conduct additional harmful data identification experiments on the MNIST, CIFAR-100, and Mini-ImageNet datasets. The results are listed as follows. Figures 6, 7, and 8 illustrate the effectiveness of the SAM-GIF algorithm in detecting and removing harmful data. The superiority of our method is demonstrated across multiple datasets. We observe that, compared to random removal, the harmful detection rate of the SAM-GIF algorithm reaches approximately 80% at a removal rate of 0.4. Moreover, by removing harmful data, the model's accuracy gradually improves.



(a) Test Accuracy (b) Harmful Data Removal

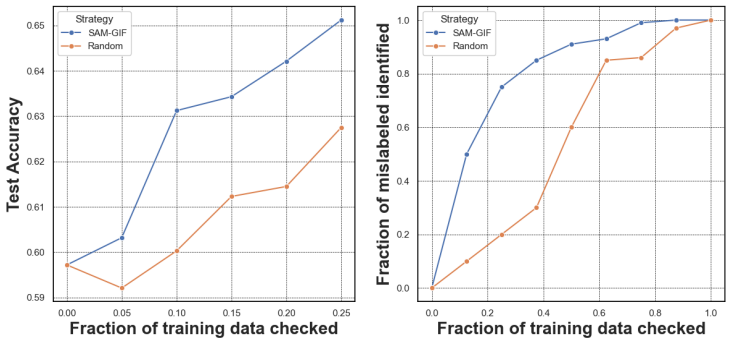
Figure 6: Harmful data removal experiment on CIFAR-100 dataset. IS: using the influence score to determine which sample to remove. Random: randomly removing tasks.

C.3 Additional Results on Interpretability

Figures 9, 10, and 11 present additional visualization results of the error prediction tracing process on the MNIST, CIFAR-100, and Mini-ImageNet datasets, respectively. The first row displays examples of misclassified test samples, the second row shows the most influential training data for classifying these samples, and the third row presents the most harmful training data for these classifications. These visualization results allow us to trace the outcomes of the error prediction process effectively.

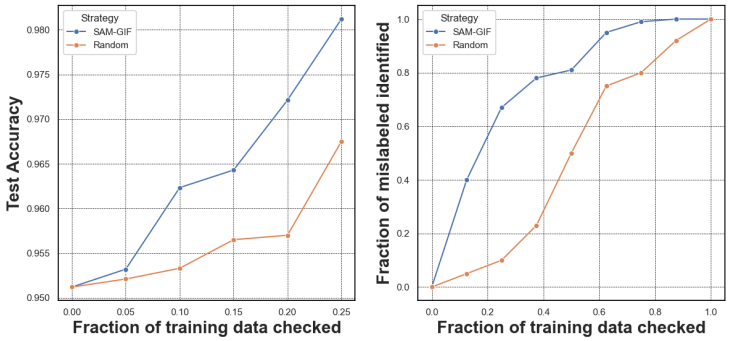
C.4 Additional Ablation Study

Figure 12 shows the ablation study results of SAM-GIF. We primarily tested the impact of different numbers of checkpoint weights on the SAM-GIF algorithm using the CIFAR-10 dataset. From the figure, we can observe that as the number of checkpoints increases, the accuracy of SAM-GIF becomes closer to that of retraining. When the number of checkpoints is 10, the accuracy of SAM-GIF is 0.9497, while the retraining accuracy is 0.9517. At the same time, as the number of checkpoints increases, the running time of SAM-GIF also increases.



(a) Test Accuracy (b) Harmful Data Removal

Figure 7: Harmful data removal experiment on Mini-ImageNet dataset. IS: using the influence score to determine which sample to remove. Random: randomly removing tasks.



(a) Test Accuracy (b) Harmful Data Removal

Figure 8: Harmful data removal experiment on MNIST dataset. IS: using the influence score to determine which sample to remove. Random: randomly removing tasks

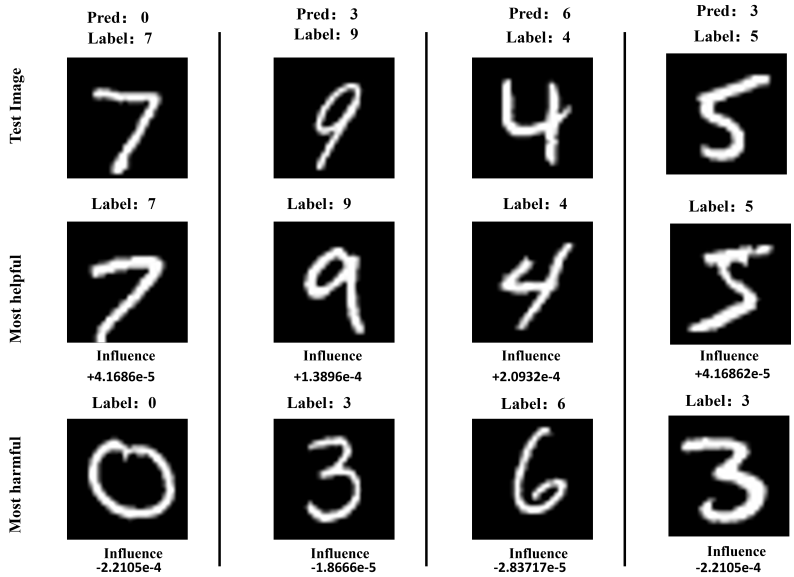


Figure 9: The most helpful and harmful training data tracked by misclassified data on MNIST dataset

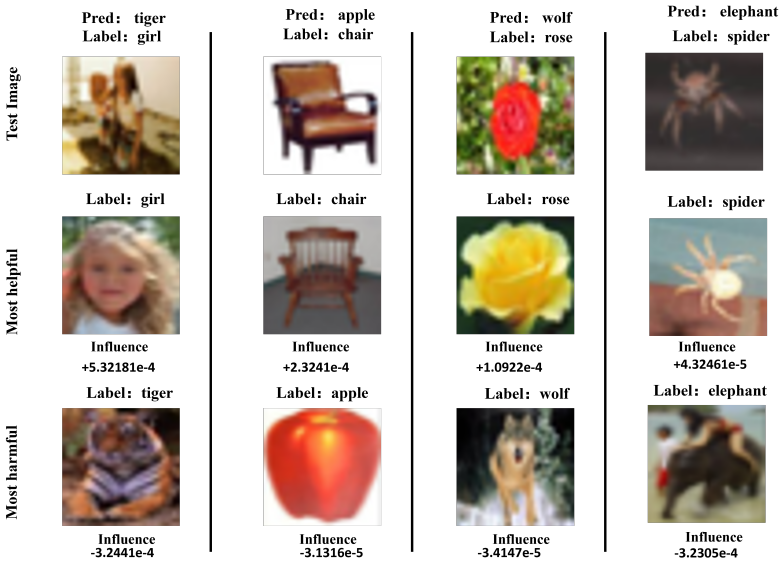
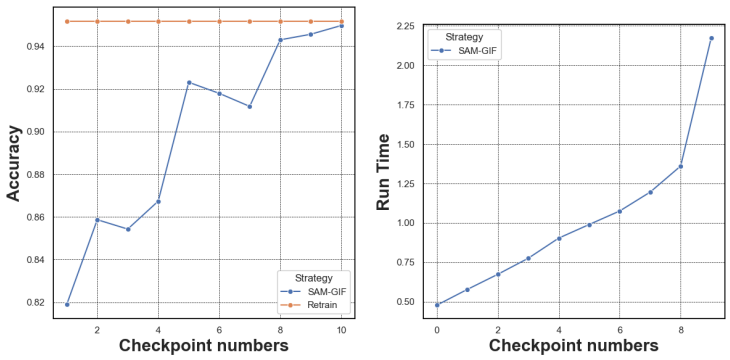


Figure 10: The most helpful and harmful training data tracked by misclassified data on CIFAR-100 dataset



Figure 11: The most helpful and harmful training data tracked by misclassified data on Mini-ImageNet dataset



(a) Accuracy of SAM-GIF (b) Runtime of SAM-GIF

Figure 12: Ablation study of SAM-GIF on Cifar10 dataset